

Dynamical System Modeling to Simulate Donor T Cell Response to Whole Exome Sequencing-Derived Recipient Peptides: Understanding Randomness in Clinical Outcomes Following Stem Cell Transplantation

Koparde V,^{*1} Abdul Razzaq B,^{*2} Suntum T,² Sabo R,³ Scalora A,² Serrano M,¹ Jameson-Lee M,² Hall C,² Kobulnicky D,² Sheth N,¹ Sampson J,¹ Roberts C,² Buck G,¹ Neale M,⁴ Toor A.²

* Equally contributing authors.

Center for Biological Complexity,¹ Bone Marrow Transplant Program, Department of Internal Medicine,
² Department of Biostatistics, ³ Department of Psychiatry and Statistical Genomics, ⁴ Virginia Commonwealth University, Richmond, Virginia.

Correspondence: Amir A. Toor MD, Professor of Medicine, Bone Marrow Transplant Program, Massey Cancer Center, Virginia Commonwealth University, Richmond, VA 23298. Ph; 804-628-2389. E-mail: amir.toor@vcuhealth.org

Word count: Abstract 385, Manuscript 9753, Figures 5, Tables 1.

Key Words: Stem cell transplantation, Whole exome sequencing, Dynamical system, Logistic Equation, minor histocompatibility antigens

Running Title: Simulating tissue-specific donor T cell responses in SCT

Abstract

The development of alloreactivity following stem cell transplantation (SCT) in HLA matched donor-recipient pairs (DRP) appears to be random. Minor histocompatibility antigens (mHA) are critical in graft versus host disease (GVHD) pathophysiology however, the quantitative relationship between GVHD and the magnitude of mHA in donor-recipient pairs (DRP) is not known. Whole exome sequencing (WES) was performed on 27 HLA matched related donors (MRD), & 50 unrelated (URD), to identify nonsynonymous single nucleotide polymorphisms (SNPs) with an average 2,490 SNPs were identified in MRD, and 4,287 in URD (p<0.01). The resulting peptide antigens that may be presented on the relevant HLA class I molecules in each DRP were derived *in silico* (NetMHCpan ver2.0) and the tissue expression of proteins these were derived from determined (GTex). MRD DRP had an average 3,626 HLA-alloreactive peptide (AP) complexes with an IC50 of <500 nM and URD, had 5,386 (p<0.01). To simulate a donor cytotoxic T cell response to these AP, the array of HLA-AP complexes in each patient was considered as an *operator* matrix modifying a hypothetical cytotoxic T cell clonal *vector* matrix in which each responding T cell clone's proliferation is quantified by the logistic equation of growth. The simulated steady state T cell clonal response to the AP-HLA complexes in each DRP, accounted for the HLA binding affinity and expression of each AP. The resulting *simulated* organ-specific alloreactive T cell clonal growth revealed marked variability between different DRP. The sum of all T cell clones for common GVHD target organs was: MRD, median 188,821 cytotoxic T cells at steady state (n=26), MUD, 201,176 (n=35), single locus HLA-mismatch MUD: 56,229 (n=10). Despite an estimated, uniform set of constants used in the model for all DRP, and a heterogeneously treated group of patients, overall there was a non-significant trend for higher organ specific T cell counts in patients with GVHD compared to those with none, with weak associations observed for GVHD of the liver. In conclusion, exome wide sequence differences and the variable AP binding affinity to the HLA in each DRP yields a large range of possible alloreactive donor T cell responses possibly explaining the random nature of alloimmune responses observed in clinical practice. Incorporating other quantitative sources of T cell response variability may allow simulations like this to accurately model alloreactivity in SCT in the future.

Introduction

Over the last four decades there have been substantial strides made in the optimizing the clinical outcomes following allogeneic stem cell transplantation (SCT). Nevertheless, outcomes such as relapse and graft versus host disease (GVHD) remain difficult to predict in individuals because of the variability observed in the incidence of alloreactivity following HLA matched SCT using conventional GVHD prophylaxis regimens. [1, 2, 3, 4, 5, 6, 7] To an extent this is also true of HLA mismatched transplantation using novel GVHD prophylaxis regimens. [8, 9] Considering that disease responses in allogeneic SCT are often linked to the development of GVHD, it is important to understand the biological basis of the randomness observed in the incidence of alloreactivity. [10] Relapse and GVHD are a function of donor-derived immune reconstitution, which shows many characteristics of a dynamical system, such as logistic growth kinetics and power law distribution of clonal frequencies. [11, 12, 13, 14, 15] This implies that if the quantitative basis of randomness in clinical outcomes can be understood in terms of donor derived immune reconstitution, it will become possible to modify the system to optimize clinical outcomes.

In HLA Matched SCT, recipient antigens, specifically, *minor histocompatibility antigens* (mHA) are presented on the HLA molecules. These mHA released following conditioning or infection induced-tissue injury are taken up by *antigen presenting cells* and presented to non-tolerant donor T cells, which in the event of antigen recognition, proliferate and home back to the target tissue initiating a graft vs. host response. Quantifying the mHA disparity in a SCT donor-recipient-pair (DRP) may therefore allow exploration of the origin of the stochastic nature of alloreactivity. It has been shown that both the magnitude and rate of recovery of donor-derived T cells influence the likelihood of relapse, GVHD and survival. [11] This indicates that T cell responses to recipient antigens may be modeled as dynamical systems, with quantitative rules that govern repertoire evolution under normal circumstances and following transplantation. T cell repertoire is exceedingly complex, it is very likely that the antigenic background will be equally as complex. Therefore the antigenic background in a DRP may be similarly described mathematically as a component of this dynamical system. These antigenic differences in a given transplant DRP may be *partially* determined using whole exome sequencing (WES) of SCT donor and recipient DNA. WES has demonstrated that there is a large library of non-synonymous single nucleotide polymorphisms (nsSNP), and an equally large array of nsSNP-derived-peptides which would have different amino acid sequences in each DRP. [16, 17] Of these nsSNPs, those present in the recipient but *absent* in the donor will in theory, yield an array of immunogenic recipient peptides which

may trigger donor T cell activation and proliferation, in other words, an array of mHA bound to the 'matched' HLA in the DRP. In aggregate these polymorphisms constitute an *alloreactivity potential* between the specific donors and recipients. In studies done to date, large magnitude of this alloreactivity potential has been observed in all the HLA matched DRP examined. When a dynamical T cell response to this mHA array is calculated marked variation in the simulated T cell response is observed, suggesting that the number and the HLA binding affinity of the mHA may determine that likelihood of alloreactivity. [18] Similar observation reporting association of polymorphisms in the peptide regions of HLA class I molecules support the premise outlined above. [19]

Nevertheless, alloreactivity is a complex clinical state, where patients may have variable manifestations of GVHD impacting different organ systems to varying extent. In this paper the impact of tissue-specific-expression of the proteins that the mHA are derived from in different individuals is examined to measure its variability between unique transplant DRP. This is done using a T cell vector-mHA operator system previously developed [18] with a uniform set of conditions employed to simulate a hypothetical CD8+ T cell response to the *in silico* derived mHA-HLA class I array in 77 HLA matched SCT DRP.

Methods.

Patients

Whole exome sequencing (WES) was performed on previously cryopreserved DNA obtained from donors and recipients of allogeneic SCT. Permission for this retrospective study was obtained from the Virginia Commonwealth University's institutional review board, and patients who underwent transplantation between 2010 and 2014 were retrospectively selected for this analysis. Patients had undergone either 8/8 (n=67) or 7/8 (n=10) HLA-A, B, C and DRB1 matched related (MRD; n=27) or unrelated (MUD; n=50) or haploidentical (n=1) SCT according to institutional standards at Virginia Commonwealth University (VCU) (Supplementary Table 1). HLA matching had been performed using high resolution typing for the unrelated donor SCT recipients; and intermediate resolution typing for class I, and high resolution typing for class II antigens for related donor recipients. A variety of different conditioning and GVHD prophylaxis regimens were used in the patients. HLA class I typing information for the donor and recipient was acquired from the clinical data base.

Whole Exome Sequencing

Nextera Rapid Capture Expanded Exome Kit was used to extract exomic regions from the DNA samples, which were then multiplexed and sequenced on an Illumina HiSeq 2500 to achieve an average coverage of ~90X per sample. 2X100 bp sequencing reads were then aligned to the human reference genome using BWA aligner. Duplicate read alignments were detected and removed using Picard tools. Single nucleotide polymorphisms (SNPs) in both the donor and recipients' exomes were determined using GATK HaplotypeCaller walker. GATK best practices were then implemented to filter and recalibrate the SNPs; and store them in variant call file (VCF) format. To identify SNPs unique to the recipient and absent in the donor the results from the GATK pipeline in VCF format were then parsed through the in-house TraCS (Transplant pair Comparison System) set of perl scripts. TraCS traverses through the genotypes of the called SNPs, systematically excluding identical SNPs or editing them to align with the graft-versus-host (GVH) direction thereby generating a new VCF with SNPs for a particular DRP in the GVH direction (SNP present in the recipient, absent in the donor).

The SNPs in this VCF are then annotated either as synonymous or non-synonymous using Annovar. The corresponding amino acid polymorphisms along with flanking regions of each protein are then extracted using Annovar to build peptide libraries of 17-mers for each DRP, with the SNP encoded AA occupying

the central position. This library is further expanded by sliding a 9-mer window over each 17-mer such that the polymorphic amino-acid position changes in each 9-mer. The HLA class I binding affinity and IC50 values, which quantify the interactions between all these 9-mers for each DRP and all six HLA class I donor molecules (HLA-A, B and C), NetMHCpan version 2.8 was run iteratively in parallel mode on a linux cluster using custom python scripts. Parsing the NetMHCpan output, unique peptide-HLA combinations present in the recipient but not in the donor, i.e., possessing a GVHD vector, were identified and organized in order of declining mHA-HLA affinity. IC50 (nM) indicated the amount of peptide required to displace 50% of intended or standard peptides specific to a given HLA. Binding affinity is inversely related to IC50, such that, smaller the IC50 value, the stronger is the affinity. The variant alloreactive peptides with a cutoff value of $IC50 \leq 500$ are included in the analyses presented here.

The Genotype-Tissue Expression (GTEx) portal V6 has publicly available expression level information (Reads/kilobase of transcripts/million mapped reads, RPKM values; <http://www.gtexportal.org/home/>) for a variety of human tissues over a large number of genes. As we know the genes from where the peptides in our DRP peptide library are originating from, we are able to parse in the RPKM values from the GTEx portal for that gene across the whole array of tissues of interest, namely, skin, lung, salivary gland, esophagus, small intestine, stomach, colon and liver. In the DRP where a male recipient had been transplanted from a female donor (n=17), full length available sequences of all proteins encoded by the Y chromosome were curated from NCBI and other resources (see supplementary material). These sequences were then computationally split into 9-mer peptides and their respective binding affinities and IC50 values for the relevant donor HLA antigens were determined in silico using the NetMHCpan software as described earlier. These peptides were then appended to the corresponding DRPs peptide library for all subsequent analyses.

Computational Methods: Dynamical System Modeling Of T Cell Response To Putative mHA

It was postulated that the immune effectors and their antigenic targets constitute a *dynamical system*, i.e. an *iterating* physical system, where the variable being studied evolves over time, and the state of any variable at any given time (t), is predicated on all the preceding states of the systems. A system demonstrating logistic growth of immune effectors may be described by the general equation

$$\frac{dN}{dt} = rN_t \left(\frac{K - N_t}{K} \right)$$

Here, dN/dt is the instantaneous rate of change of the cell population at time t , when the population N_t has an intrinsic growth rate, r and a maximum size, K . This logistic dynamical system constitutes a system of repeated calculations, where the output of the equation for each iteration gives the population N_t , as a *function* of time, and becomes the input variable (*argument*) for the next calculation N_{t+1} . This system behaves in a *non-linear* fashion, demonstrating sigmoid population growth constrained by feedback. [18, 20, 21]

If SCT is considered as a system of interacting donor T cell clones and recipient antigens, immune reconstitution following SCT may be modeled mathematically. Each T cell clone responding to its target antigen will proliferate, conforming to the *iterating logistic equation* of the general form

$$N_t = \frac{K}{(K - N_{t-1})(e^{-rt}) + 1} \quad [1]$$

In this equation: N_t , is the T cell count at time t following transplant (modeled as iterations); N_{t-1} represents the T cell count in the previous iteration; K is the T cell count under steady state conditions reached after several iterations, and represents the maximum T cell count the system would support (carrying capacity); r , is the growth rate of the population; and t is the number of iterations that the population has gone through (representing time). T cell population, N_t , at time, t following SCT, is a function of the T cell population N_{t-1} , at an earlier time point, $t-1$. This in turn will depend on the T cell population at the outset of transplant N_0 , and the intrinsic T cell proliferative capacity (growth rate) r governing the growth, such that

$$N_0 \xrightarrow{[r]} N_{t-1} \xrightarrow{[r]} N_t \xrightarrow{\dots [r]} K$$

In this model, the final steady state population of all the T cell clones (n) ($\sum_1^n K$), and its clonal repertoire may be studied for associations with clinical outcomes.

Matrices To Model The T Cell Clonal Repertoire: Vector Spaces And Operators

To apply the logistic equation to describe the evolution of all the individual T cell clones present in an individual at a given time, in other words, to *simulate* the evolution of the T cell clonal repertoire responding to the entire WES derived mHA-HLA library for an individual DRP, matrices are utilized. T cell clones present in an individual may be considered as a set of individual *vectors* in the immune *phase*

space of that individual. The descriptor, *vector*, in this instance is used to describe the entire set of T cells, with the individual T cell clones representing components of this vector [22]. In this vector, T cell clonality represents direction (since it determines antigen specificity) and T cell clonal frequency, the magnitude of individual vector components. The sum of these vectors will represent the overall T cell vector and its direction, in this simulation, recipient-directed alloreactivity. The T cell vectors may take a number of different configurations in an individual, and the entire range of possible vector configurations will constitute the *immune phase space* for that individual. The T cell vector may be represented mathematically as a single row matrix, with T cell clonal frequencies $TC_1, TC_2, TC_3 \dots TC_n$. This T cell clonal matrix may be represented by the term, $\overline{v_{TCD}}$. The frequency of each TC is a natural number, and the direction, its reactivity, represented by the clonality. Phase space will then describe all the potential T cell clonal frequency combinations possible, within a specific antigenic background, with all the potential directions of the T cell reactivity. In the case reported here, the vectors are all in the direction of graft vs. host alloreactivity, since they proliferate after encountering mHA-HLA. In contrast, the infused T cell clonal repertoire will represent a steady state T cell clonal frequency distribution in the normal donor, presumably made up of mostly self-tolerant, pathogen specific T cells, and without any auto-reactive T cells. For the computations reported here, each T cell clone has a N_0 value of 1, and is alloreactive.

The T cells infused with the transplant encounter a new set of antigens (both recipient and pathogen). These antigens presented by the recipient (or donor-derived) antigen presenting cells constitute an *operator*, a matrix of targets in response to which the donor T cells may proliferate [23]. This operator changes the magnitude and direction (clonal dominance) of the infused T cell repertoire, as individual T cell clones in the donor product grow or shrink in the new HLA-antigen milieu, transforming the T cell vector. The putative mHA making up the alloreactivity potential constitute a matrix, which may be termed an *alloreactivity potential operator*, \mathbb{M}_{APO} . This operator will consist of the binding affinity of the unique variant peptide-HLA complexes likely to be encountered by donor T cells in an individual recipient. Following SCT, the donor T cell clonal frequency shifts according to the specificity of the TCR and the abundance and reactivity of the corresponding antigen. This corresponds to the operator modifying the original donor T cell vector, $\overline{v_{TCD}}$ as the system goes through successive iterations to a new recipient T cell vector, $\overline{v_{TCR}}$, according to the following relationship

$$\overline{v_{TCD}} \cdot \mathbb{M}_{APO} = \overline{v_{TCR}} \quad [2]$$

Applying the Logistic Growth Equations to Vector-Operator Systems

A central assumption in this model is that the steady state TC clonal frequency (K) of specific TCR bearing clones, and their growth rates (r), are proportional to the binding affinity of their target mHA-HLA complexes. This is *approximately* represented by the reciprocal of the $IC50$ (test peptide concentration in nM required to displace a standard peptide from the HLA molecule in question) for that specific complex. This is because the strength of the binding affinity will increase the likelihood of T cell-APC interactions occurring, thus influencing the driving the rate of this interaction. While each TCR may recognize another mHA-HLA complex with equal or lesser affinity, for the sake of simplicity, an assumption of non-recognition of other mHA-HLA complexes was made for this model. This makes it possible to specify an *identity matrix*, Matrix A, with unique mHA-HLA complexes for a SCT-DRP and the corresponding TCR, where TCR_x recognizes mHA_x -HLA (1) and not others (0). In addition to the assumption that there is a first signal of TCR recognition, a second signal immune responsiveness is assumed in this matrix.

Matrix I. Effect of alloreactivity operator M_{APO} on T cell vector $\overline{v_{TCD}}$. Successive iterations (t) modify the vector to $\overline{v_{TCR}}$. In this simplified model, mHA_x -HLA only effects TC_x and so on. Matrix below represents a single iteration t .

SCT	M_{APO}				
		mHA ₁ HLA	mHA ₂ HLA	mHA ₃ HLA	mHA _n HLA
$\overline{v_{TCD}}$	TC_1	1	0	0	0
$\downarrow t$	TC_2	0	1	0	0
$\overline{v_{TCR}}$	TC_3	0	0	1	0
	TC_n	0	0	0	1

The *alloreactivity matrix* modifies the donor T cell clonal vector infused with an allotransplant, mapping it to the recipient T cell vector, as the T cell clones with unique TCR encounter the corresponding mHA-HLA complexes they proliferate conforming to the logistic equation [1]. In the logistic equation K for each T cell clone will be proportional to the approximate binding affinity ($1/IC50$) of the corresponding mHA-HLA complex ($K^{1/IC50}$). The parameter r is a function of the binding affinity (by increasing the TCR-mHA-HLA interaction time) and the intrinsic T cell proliferation capacity. Equation 1 must therefore be modified for unique TC clone TC_x , responding to mHA_x -HLA, as follows:

$$N_t TC_x = \frac{K^{1/IC50mHAx}}{(K^{1/IC50mHAx} - N_{t-1} TC_x)(e^{-rt(1/IC50mHAx)}) + 1} \quad [3]$$

This general equation gives instantaneous T cell counts in response to antigens presented, regardless of tissue distribution. In the alloreactivity, vector-operator identity matrix, the values 1 or 0 in each cell are multiplied by the product of equation 3 for each T cell clone. This is depicted in Matrix II.

Matrix II. Matrix illustrating a single iteration of the alloreactivity operator M_{APO} on T cell vector $\overline{V_{TCD}}$. Each cell in the matrix calculates the value of TC_x in response to mHA_x -HLA, final repertoire is determined by solving the matrix.

SCT		M_{APO}			
		mHA ₁ HLA	mHA ₂ HLA	mHA ₃ HLA	mHA _x HLA
$\overline{V_{TCD}}$ $\downarrow t$ $\overline{V_{TCR}}$	TC_1	$N_t TC_1 = \frac{K^{1/IC50mHA1}}{(K^{1/IC50mHA1} - N_{t-1} TC_1)(e^{-rt(1/IC50mHA1)}) + 1}$	0	0	0
	TC_2	0	$N_t TC_2$	0	0
	TC_3	0	0	$N_t TC_3$	0
	TC_x	0	0	0	$N_t TC_x$

The T cell response to each mHA-HLA complex is determined over time, t , by iterating the system of matrix-equations. In this *alloreactivity matrix*, the IC50 of all the alloreactive peptides with a GVH direction (present in recipient, but absent in donor) constitutes the operator; the sum of n T cell clones $\sum_1^n TC$, at each time point will represent the magnitude of the vector $\overline{V_{TCR}}$ at that time t . In this system, when considering the effect on infused donor T cell vector, depending on antigen affinity, T cell clones present in abundance may be down-regulated if antigen is not encountered. On the other hand, clones present at a low frequency may expand upon encountering antigen, *transforming* the vector over time from the original infused T cell vector. In summary, the alloreactivity operator determines the change in donor T cell vectors, following transplantation, in an iterative fashion *transforming* it to a new configuration, over time t , based on the mHA-HLA complexes encountered in the recipient and their affinity distribution (*and antigen abundance, vide infra*). Therefore post-SCT immune reconstitution may be considered as a process in which T cell clonal frequency vectors are iteratively multiplied by the minor histocompatibility antigen matrix operator and this results in transformation of the vector over time to either a GVHD-prone alloreactive or to a tolerant, pathogen-directed vector. This may be visualized as thousands of T cell clones interacting with antigen presenting cells, an example of an interacting dynamical system. [11]

Competition between T Cell Clonal Populations

Each of the T cell clones is behaving like a unique population, therefore *competition* with other T cell clones in the set of all T cell clones must be accounted for in the logistic equation to determine the magnitude of the unique clonal frequencies as the model iterates simulating T cell clonal growth over time. This may be done using the *Lotka-Volterra* model for *competing populations*, which accounts for the impact of population growth of multiple coexisting populations [18, 24, 25]. This is accomplished by modifying the expression N_{t-1} in equation 3 for each clone, by taking the sum of N_{t-1} for all the other competing T cell populations when calculating N_t for each clone. Each clone's N_{t-1} is weighted by a correction factor α for its interaction with the T cell clone being examined. Given the central role for the target mHA-HLA complex's $IC50$ in determining the T cell frequency for each clone, α for each clone is calculated by dividing the $IC50$ of the competing T cell clone with the test clone (note the use of $IC50$ instead of $1/IC50$). This implies that T cell clones recognizing mHA-HLA complexes with a higher binding affinity will have a disproportionately higher impact on the growth of T cell clones binding less avid mHA-HLA complexes and vice versa. The resulting square matrix, Matrix III, will have 1 on the diagonal, and values <1 above the diagonal and >1 below it.

Matrix III. Matrix illustrating the relative effect of antigen binding affinity on the T cell clonal interaction between different clones. Successive cells in each row of the matrix calculate the effect of TC_i on T cell being studied, TC_x . This generates a weighting factor, α , which modulates the impact of population of TC_i on the growth of TC_x .

	TC_1	TC_2	TC_3	TC_n
TC_1	$IC50_1/IC50_1$	$IC50_1/IC50_2$	$IC50_1/IC50_3$	$IC50_1/IC50_n$
TC_2	$IC50_2/IC50_1$	$IC50_2/IC50_2$	$IC50_2/IC50_3$	$IC50_2/IC50_n$
TC_3	$IC50_3/IC50_1$	$IC50_3/IC50_2$	$IC50_3/IC50_3$	$IC50_3/IC50_n$
TC_n	$IC50_n/IC50_1$	$IC50_n/IC50_2$	$IC50_n/IC50_3$	$IC50_n/IC50_n$

To account for n competing T cell populations, equation 3 will be modified as follows

$$N_t TCx = \frac{K^{1/IC50mHAx}}{(K^{1/IC50mHAx} - \sum_1^n N_{t-1} TCi \cdot \alpha_i)(e^{-rt(1/IC50mHAx)} + 1)} \quad [3.1]$$

Where for the T cell clone x , N_t depends on the sum of the n T cell clonal frequencies at the previous iteration, with the α of each T cell clone i , with respect to the T cell clone x , modifying the effect of the frequency of the i th clone on TCx . By contrast, the parameter r can have either positive or negative values depending on whether the ambient cytokine milieu, either stimulates ($-r$) or suppresses ($+r$) growth.

The direction of the T cell clones will be determined by antigen specificity, i.e. whether their TCR recognize the recipient's mHA-HLA (are alloreactive) or not (are tolerant), such as pathogen directed T cell clones. For example, a tolerant, non-autoreactive set of T cell clones (donor vector, $\overline{V_{TCD}}$) may be transformed to a predominantly alloreactive set of T cell clones ($\overline{V_{TCR}}$), after interacting with the mHA-HLA complex, alloreactivity operator encountered in the recipient (\mathbb{M}_{APO}).

Accounting for tissue expression of proteins

The peptides discussed in the afore mentioned derivation are generated from proteins expressed in target tissues, as such the level of protein expression will determine the magnitude of the peptide specific T cell response. The higher the protein expression, the more peptide molecules and the greater the HLA presentation with an ability to stimulate a larger T cell response (clonal frequency). Therefore the parameter K in the above equations may be modeled as a multiple of the level of protein expression. The tissue expression of proteins is estimated by RNA sequencing techniques, and is measured in either transcripts per million (TPM) or reads per kilobase of transcript per million mapped reads (RPKM). The values available from the public data base GTEx, range from 0 to $>10^4$ and constitute a coefficient in the definition of K . This Modifies Equation 3.1,

$$N_t TCx = \frac{(RPKM_x \cdot K)^{1/IC50mHAx}}{((RPKM_x \cdot K)^{1/IC50mHAx} - \sum_1^n N_{t-1} TCi \cdot \alpha_i)(e^{-rt(1/IC50mHAx)} + 1)} \dots [3.2]$$

In equation 3.2, the tissue expression of the protein from which the target peptide, $mHAx$ is derived is incorporated as a K multiplier when calculating a tissue-specific T cell response. Thus tissue-specific alloreactivity potentials may be simulated for each of the relevant GVHD target tissues, by substituting equation 3.2 into Matrix II.

In applying this model to exome sequence derived, alloreactive-peptide-HLA binding patient data an IC50 cutoff value of ≤ 500 nM, and an RPKM value of ≥ 1 were chosen to study the differences between

patients. The T cell repertoire simulations were then run in MATLAB (Mathworks Inc., Natick, MA), utilizing the above model (See Supplementary Mathematical Methods and Program).

The sum of all T cell clones $\sum_1^n TC$ for each specific organ of interest and the grand total of the organs studied (termed sum of all clones) were used to represent the T cell vector magnitude of the alloreactive T cells at steady state for each patient.

Statistical Methods

Estimated T cell counts are summarized per organ and in total with means and standard deviations, both overall and by GVHD classification. In addition, variability measures of estimated T cell counts across organs within individuals (standard deviation, minimum, maximum, and range) are summarized in the same manner. The estimated T cell counts and variability measures are compared between GVHD and Donor Type groups using the Wilcoxon rank sum test. Cox proportional hazards models are used to examine associations between both the estimated T cell counts and variability measures with patient outcomes (GVHD, survival, relapse and relapse-free survival). The MEANS, NPAR1WAY and PHREG procedures in the SAS statistical software program (version 9.4, Cary, NC, USA) are used for summaries and analyses. All estimated T cell counts are divided by 1000 to simplify the presentation of results.

Results.

Exome sequencing

Cryopreserved DNA samples from 78 donors and recipients of allogeneic SCT were sequenced, demographic details of the patients are given in supplementary table 1. Whole exome sequencing revealed a significantly larger number of SNPs, both synonymous as well as non-synonymous in recipients of MUD SCT when compared with MRD recipients (Table 1). Further, a majority of these SNPs were nonconservative, i.e. likely to substitute an AA with different physico-chemical properties, so liable to bring about a conformational change. In patients who either did or did not develop GVHD, an average of 2456 and 2474 nsSNPs were identified in recipients of MRD, while the corresponding numbers for MUD recipients were 4536 and 3845 nsSNPs. In the one haploidentical transplant recipient, there were 3231 ns SNPs. Notably, the transition/transversion ratio in the WES data was as expected between 2.1 and 2.5 for the entire data set (Supplementary Fig 1).

In silico derivation of mHA-HLA complexes from exome variation

The nsSNP_{GVH} data arrays then served as the basis to computationally determine peptide sequences. For each variant amino acid (AA) resulting from a nsSNP_{GVH}, the flanking 8 AA on either side were determined and the resulting nonamers, with the variant AA occupying all nine positions derived for each variant AA. The binding affinity of each of these peptides was determined to the HLA class I (A, B and C) molecules in each pair. This yielded a large array of unique peptide-HLA complexes, in other words *putative* or *potential* minor histocompatibility antigens (mHA) in each individual; once again a significantly larger number of peptides of both presented and strongly bound, were observed in MUD recipients when compared with MRD (Table 1). A similar number of peptides with an IC50 <500nM, 3826 and 3406 pmHA, were recorded in MRD patients either with or without GVHD respectively; corresponding numbers were 895 and 778 mHA with an IC50 <50nM for those patient groups. For the MUD SCT pairs (n=50), the corresponding numbers were 5672 and 4876 pmHA with an IC50 <500 nM and 1210 and 1071 with an IC50 <50 nM in patients with or without GVHD. Notably these numbers do not include the Y chromosome derived peptides presented by the class 1 HLA molecules in male recipients of female donors. The haploidentical donor had 2448 peptides with an IC50 of <500 nM out of a total 57957 peptides; of these 484 were strongly bound, when using the recipient HLA for performing the calculation.

Simulating recipient tissue specific donor T cell responses

Following determination of the mHA with various binding affinity distributions, the T cell responses to these antigens were simulated using the T cell vector- alloreactivity operator model [Equations 2 & 3.2]. The underlying conditions used in these calculations were as follows: for each mHA there was a single T cell present at the first iteration, i.e. $N_t = 1$ at $t = 1$. The K in equation 3.2 was set at 1000,000 cells (note: this value substitutes for organ mass, lympho-vascular supply etc. without accounting for differences between organs), and r was set at 1.5 for all the simulations (note: in vivo this may vary with state of inflammation). All the mHA were included in the simulations with competition, and included Y chromosome encoded peptides which bound respective HLA in the male recipients of female donors. The program accounted for both IC50 and tissue expression measured as RPKM for each mHA to simulate donor T cell responses to organs of interest, with skin, salivary gland, esophagus, stomach, small intestine, colon, liver, spleen, blood, blood vessel, lung included in the analysis. Individual clonal growth was variable depending on the HLA binding affinity of the peptide, as well as the tissue expression of protein, however the relationship was not linear (Figure 2). T cell clones responding to low expression/low binding affinity were suppressed and had negative values and recovered over time (iterations of the system). The T cell clonal growth for each organ's alloreactive peptides was summed to give the simulated alloreactive T cell count for each organ in each individual. The average value for each organ at steady state (average of the iteration # 401-500) was determined and is shown for each patient (Figure 3A) and depicts the magnitude of organ-specific alloreactive T cell response that may be seen in different DRP, accounting for their HLA types and exome sequence variation. The simulated organ-specific T cell counts responding to the alloreactivity operator demonstrate marked variability in both HLA matched related and unrelated donors, both between different DRP (Figure 3B) as well as within DRP (Figure 3C). This is true for individual organ simulations, as well as the sum of these simulations (Figure 3D), which reflects the variation in the organ specific T cell responses.

When the sum of all organ specific T cell clones (Σ TC) was examined in different donor types, no significant differences were observed in any of the categories examined; MRD: median 188,821 Σ TC at steady state (n=26) vs. MUD: 201,176 (n=35) vs. HLA mm donor: 56,229 (n=10). However, while the differences were not statistically significant between these retrospectively chosen groups, there was a trend supporting quantitative differences between different donor types. Estimated T cell counts are summarized by donor type in Supplementary Table 2, where for every organ (and overall) the mean expected T cell counts and estimated variabilities are larger in patients with unrelated donors than they

are in patients with matched related donors, however none of these differences were significant (all p-values > 0.3), most likely due to the high variability of these estimates. No significant differences were observed when other biological features such as gender mismatch in the DRP (F to M: 270,613 (n=17), M to F: 135,064 (n=14) vs. gender match (F to F: 180,574 (n=16), M to M: 114,932 (n=26), and difference in races, (AA to AA: 113,245 (n=13), vs. C to C: 215,337 (n=47), vs. race mm: 57,938 (n=6)) were studied. This corroborates well with the relatively weak effect of these biological differences in the development of GVHD in the setting of HLA matching. [26, 27] However the small sample size and heterogeneity of our group in terms of conditioning and GVHD prophylaxis may also contribute to the variability observed in clinical outcomes.

Clinical association of tissue-specific alloreactivity potential

The simulated T cell counts are summarized in Supplementary Table 3, where for every organ (and overall) the mean simulated T cell counts were larger in patients who eventually developed any form of GVHD, than they were in patients who did not develop GVHD, though none of these differences were significant. As can be seen in Supplementary Table 4, that while none of the organ-specific simulated T cell counts were associated with GVHD (all p-values between 0.05 and 0.15), the variability (standard deviation) among organ-specific T cell estimates in individuals is significantly associated (HR = 1.08, 95% CI: 1.01, 1.15, p = 0.0275) with GVHD, as was the maximum organ-specific T cell estimate (HR = 1.01, 95% CI: 1.00, 1.02, p-value = 0.0462) and the range between the maximum and minimum organ-specific t-cell counts (HR = 1.02, 95% CI: 1.00, 1.05, p-value = 0.0276). These results imply that increased variability of T cell counts among organs are associated with a minimal increase in the risk of GVHD. Similar analyses for survival, relapse and relapse-free survival were not significant for any of the organ-specific T cell counts or the variability measures (all p-values > 0.5). While these are weak associations at best, it is noteworthy that despite an estimated, uniform set of constants used in the model for all DRP, heterogeneously treated group of patients, overall there was a trend for higher organ specific T cell counts in patients with GVHD compared to those with none.

Cox proportional hazards models for acute and chronic GVHD are presented in Supplementary Table 5, and demonstrated no significant associations between expected t-cell counts and variability measures with acute GVHD (all p-values > 0.05). For chronic GVHD, only the expected T cell counts from the liver were significantly associated, with a slight positive relationship (HR = 1.01, 95% CI: 1.00, 1.03, p-value = 0.0411). The standard deviation among organ-specific t-cell estimates is significantly (p = 0.0404) and

positively associated (HR = 1.08, 95% CI: 1.01, 1.16) with GVHD, as was the range between the maximum and minimum organ-specific T cell counts (HR = 1.03, 95% CI: 1.01, 1.05, p-value = 0.0266). These results imply that increased variability of t-cell counts among organs are associated with slight increases in the risk of chronic GVHD.

There were no associations between organ-specific expected T cell counts and the organ-specific occurrence of acute GVHD (all p-values > 0.5). Only expected T cell counts in salivary glands was significantly and positively associated with oral chronic GVHD (HR = 1.02, 95% CI: 1.01, 1.04, p = 0.0131); all other organ-specific expected t-cell counts were not associated with organ-specific chronic GVHD (p-values > 0.09).

Discussion.

Alloreactivity following SCT is a complex disorder dependent on a number of factors such as degree of HLA matching, [28, 29, 30] intensity of immunosuppression [31, 32, 33] and the graft source/T cell composition of the graft. [34, 35] However, even within uniformly HLA matched and immunosuppressed patients with similar disease biology, outcomes remain variable and subject to laws of probability. In this paper the magnitude of difference in putative alloantigen presentation between SCT DRP is explored, accounting for the HLA make up and protein coding differences between individual donors and recipient. Marked variation in the likelihood of alloantigen presentation is observed in the simple mathematical model utilized. Further despite the limited nature of the model used, a trend supporting association of the alloreactive simulations with clinical GVHD is observed.

Logically, the binding affinity and tissue expression of the antigens are critical parameters when assessing the T cell response to these antigens. In this paper findings of an earlier model are extended to simulate T cell responses to the entire array of alloantigens that the donor T cells may encounter in a recipient to determine tissue specific alloreactivity potential. Similar to the previous study, the findings reported herein demonstrate a very large degree of variability between the simulated T cell responses to antigens expressed in specific organs between unique pairs. Furthermore, while the association between clinical GVHD and the simulated T cell responses is not established, there are intriguing associations observed which represent a new area of investigation which might yield interesting results in the future.

The inability to identify strong clinical association between the magnitude of the simulated T cell response to mHA array in a DRP and GVHD, may be explained by, (a) uniform simulation conditions applied in the model, despite a heterogeneously treated patient cohort, with limited numbers in each group, (b) only 9-mer oligo peptides bound to HLA class I considered in the simulations, and those too without any post translational modification (phosphorylation, glycosylation) and protein cleavage site information incorporated. Beyond these obvious considerations there are other important considerations that needs to be factored in. Logic would dictate that when proteins are cleaved, there will be a host of peptides generated for antigen presentation, both alloreactive, such as the ones reported here, as well as non-alloreactive peptides which will also bind HLA with varying levels of affinity, as the alloreactive peptides do. Furthermore these peptides will likely be far more numerous than the alloreactive ones, and may constitute a significant competitive barrier to the presentation of

alloreactive peptides. This may be modeled numerically using the notion of *combinatorial probability*. [36, 37] In other words, if there are n total peptides which might be presented on k HLA molecule there are,

$$\binom{n+k-1}{k} = \frac{n+k-1!}{k!(n-1)!}$$

possible combinations of peptides which might be presented by these HLA molecules, including duplication of peptides and without regard to order of peptides presented. For example, if 10 peptides are to be presented by 4 HLA molecules the total number of possible peptide-HLA combinations will be, $\binom{13}{4} = 715$. Now, of these, if 3 peptides are alloreactive (mHA), the probability of a favorable outcome (NO GVHD) will be enhanced if the other 7 non-alloreactive peptides are presented, the number of possible combinations allowing that will be $\binom{10}{4} = 210$. Therefore the probability of having a peptide combination presented by one of the four HLA molecules, which will not include an alloreactive peptide in this mix of 3/10 alloreactive peptides, will be approximately

$$\frac{\binom{10}{4}}{\binom{13}{4}} = 0.293$$

This means that the remaining ~70% of the peptide-HLA combinations will contain one or more alloreactive peptides, if this combination of alloreactive and non-alloreactive peptide combinations were to be presented. Depending on the binding affinity of the peptides, and the potential of the alloreactive peptide to stimulate a T cell response, and the presence of a T cell clone recognizing that specific peptide HLA combination, alloreactivity may or may not be triggered. In real life however the number of non-alloreactive peptides is likely high resulting in a smaller ratio of alloreactive peptides being presented. Expression levels of HLA molecules (k in the above equations) have been shown to impact alloreactivity in, supporting this quantitative reasoning. [38, 39] Nevertheless this quantitative consideration adds an important variable to determining the likelihood of alloreactivity developing; i.e. the variability in the HLA binding affinity of the many non-alloreactive peptides (not accounted for in the analysis presented in this paper). Further variability in this system is introduced by the relative abundance of each protein from which the peptides are derived. This too will modify the likelihood of peptide binding to HLA, due to competition. This discussion demonstrates that while dynamical systems modeling reproduces T cell patterns seen in patients, randomness of the exome mutations, and subsequent peptide-HLA interactions makes the development of alloreactivity a *stochastic*, dynamical process. This means that while patterns of reactive immune responses may be mathematically described, each of these patterns is associated with a certain probability of occurring and thus bringing

about the associated clinical outcome. In other words, HLA matched patients with a higher simulated T cell count will likely be at greater risk of GVHD under certain uniform conditions of immunosuppression and vice versa.

Another source of difference between an idealized simulation and the 'real world' will be the interaction between APC and T cells. Both the cell populations proliferate in response to inflammatory stimuli, with the APC proliferation driving T cell growth. This interaction too may be modeled, using the matrix based vector operator model. The results reported above are based on the notion that the APC matrix operator (\mathbf{M}_{APC}) has a constant effect of the donor T cell vector, in other words antigen presentation is a constant function of time, however in life this is not the case. APC themselves respond to inflammatory signals and as previously demonstrated follow logistic growth and decline after stem cell transplantation, consequently antigen presentation follows a crescendo-decrescendo course over time (particularly with infections). [40, 41] This model may be built into this system of vector operator immune response modeling. In this instance consider the scenario; tissue injury following conditioning therapy ensues, following which there is uptake of recipient antigens by the transplanted APC (presumably of donor origin) proliferating in response to the cytokines released as a consequence of the insult. The proliferating APC take up antigen and present the mHA (and non-mHA) and migrate to the regional lymph nodes. As these monocyte populations arrive in the regional nodes, the T cells corresponding to the mHA start proliferating and migrate out of the lymph node and homing to the target tissue, where they now induce further inflammatory injury, further expanding the APC proliferation, until the APC population reaches a steady state. Once the tissue damage is complete (or infection resolved), the APC will decline and a steady state memory T cell complement left behind. This is a positive feed back loop which 'self regulates' as steady state values are reached for the APC population, with an eventually decline in the antigen presentation (as pathogen numbers decline, or maximal tissue injury runs its course). Similar to T cell clonal proliferation, APC proliferation may be described by equation 1. The progressive rise and fall in the number of APC, (and consequent waxing and waning antigen presentation over time) may then be described as a vector, and its impact in T cell population be recorded by taking the dot product of this and the T cell vector, in other words multiplying each iteration of the T cell vector as it transforms. The logistic variable describing the impact of APC growth and decline on T cell clonal proliferation is given by the expression,

$$v_{APC} = \left(1 - \left(\frac{N_{tAPC}}{K_{APC}} \right) t \right) + 1$$

This variable is at its highest value, 2, in the beginning of the reaction (N_{tAPC}/K_{APC} approaches 0) but as the reaction proceeds over time t , it approaches 1, as N_{tAPC} approaches K_{APC} . Here 1 represents the binary (0/1) condition of T cell clone specificity for target mHA in M_{APO} , in real world terms the steady state capability of the T cell to proliferate when encountering the relevant antigen. Assuming that an independent v_{APC} exists for each antigen in the M_{APO} , the effect of APC growth and subsequent mHA presentation may be obtained by the dot product of the two vectors, v_{APC} and v_{TCR} . In other words, multiplying each iteration of the T cell vector with each iteration of this APC vector (the operation of multiplying 2 column matrices), transforms the donor T cell vector,

$$v_{TCR}' = v_{TCR} \cdot v_{APC} \cdot \cos\theta$$

This equation implies that in the beginning of an inflammatory response there is a positive feedback response from proliferating APC, which amplifies the T cell response v_{TCR}' ; eventually both decay to a steady state level. The angle θ between the two vectors is 0° ($\cos 0 = 1$) because they have the same direction, in other words the TCR recognize the mHA-HLA complex being presented by the APC. This effect of v_{APC} on v_{TCR} can be applied to the entire T cell repertoire and is shown in Figure 4A for a single T cell clone and may be generalized to the whole repertoire (Figure 4B). As can be seen these graphs recapitulate the T cell response amplification commonly observed in response to antigen stimulation, [40, 41, 42] and can be depicted in the model illustrated in Figure 4C. In practice, this interaction depending on the presence or absence of inflammation in the tissues being studied, will significantly modify the alloreactivity operator and lead to variability in T cell proliferation observed. The weak associations of the T cell simulations with the clinical findings reported in this paper, may therefore be explained by absence of information regarding the overall inflammatory state in each DRP. This can certainly be modeled in the future iterations of such work.

Another source of clinical variability that is not accounted for in this model is the make up of the graft both in terms of effector, as well as regulatory T cells (Treg). While the notion of absence of antigen directed clonal T cells impacting the predictive power of any such model is straight forward, the effect of regulatory immune cell populations such as Treg requires some calculation to understand. Treg recognize self-antigens and secrete anti-inflammatory cytokines (IL-4, IL-10) in response, diminishing the proliferation of the antigen directed CD8+ effector T cells. [43] This may be easily accounted for in this model by considering that the growth parameter r (given the uniform value of -1.5 in this analysis) represents the proliferative effect of the cytokine milieu. In this instance the more negative its value

(induced by pro-inflammatory cytokines), the larger the growth promoting effect, and the less negative or positive the value (anti-inflammatory cytokine effect) the more growth will be impeded or stopped, as can be seen in Figure 5, where a change in the magnitude of r produces dramatic decline in the T cell growth curves. Once again these effects are not accounted for in the model presented here but may be easily included. Nevertheless, the robustness of the vector operator model of quantifying T cell response and its eventual clinical utility are indicated by its robustness in quantifying a variety of immune phenomenon noted above.

Current clinical practice to identify donors is based on the degree of major histocompatibility locus matching. Based on this, immunosuppressive regimens are chosen; unrelated donor transplant recipients frequently receive ATG in addition to the standard calcineurin inhibitor + methotrexate, haploidentical transplant recipients receive post transplant cyclophosphamide and so on. In the absence of early GVHD onset, immunosuppression intensity is gradually reduced and eventually withdrawn over a predetermined period of time, usually spanning four to six months, depending on the relapse risk of the underlying malignancy. Dynamical system modeling of immune reconstitution, based on whole exome sequencing data from donors and recipients may enable the development of patient specific immunosuppressive regimens post transplant, by more precisely calibrating the GVHD risk that unique donors might pose to that patient. Given the advances in *next generation sequencing*, as well as computing technology it is conceivable that in time patients and their prospective donors will have their HLA type and alloreactivity potential determined by whole exome sequencing. A donor with optimal alloreactivity potential will be identified and a GVHD prophylaxis regimen of optimal intensity utilized to achieve maximal *likelihood* of good clinical outcome. In so doing, dynamical systems understanding of alloimmune T cell responses will *attenuate* the unpredictability that the current largely probability based models of outcomes prediction expose patients to. The dynamical systems analysis of antigenic variation also explains the randomness at hand in human immune response to disease, either infectious or neoplastic. This understanding has the potential to impact areas of investigation beyond transplant alloreactivity, potentially influencing cancer immunotherapy, autoimmune disease and infectious disease. Randomness within the dynamical system will remain a problem for the foreseeable future, but a model such as this is a step towards gaining a quantitative understanding of complex immune responses.

In conclusion this model partially explains why immune responses are seemingly random and difficult to accurately predict, akin to the quantum uncertainty principle, you can accurately measure either a

particle's position or its velocity, never both. Similarly, given the complexity at hand in immune responses, we will not be able to precisely quantify the likelihood of alloreactivity, but with a quantitative understanding give a more accurate estimate of the probability distribution.

Figures.

Figure 1. TRaCS, computational algorithm to determine tissue specific alloreactive peptide mHA.

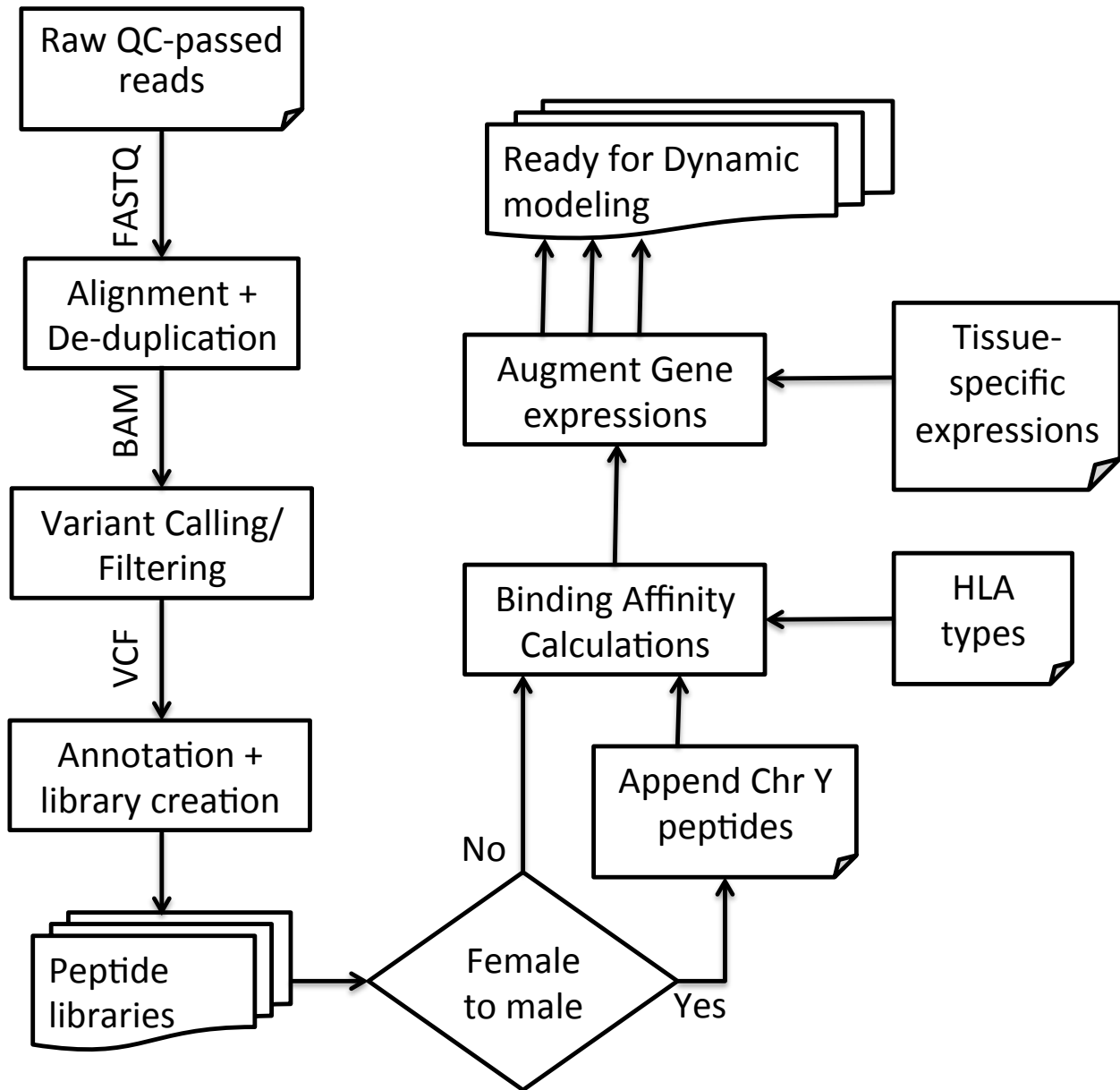


Figure 2. Individual T cell clonal growth simulations accounting for peptide-HLA complex binding affinity and protein of origin RPKM. Increased T cell frequency (Y-axis) seen if the protein is expressed at a higher level. IC50/RPKM given for each T cell clone.

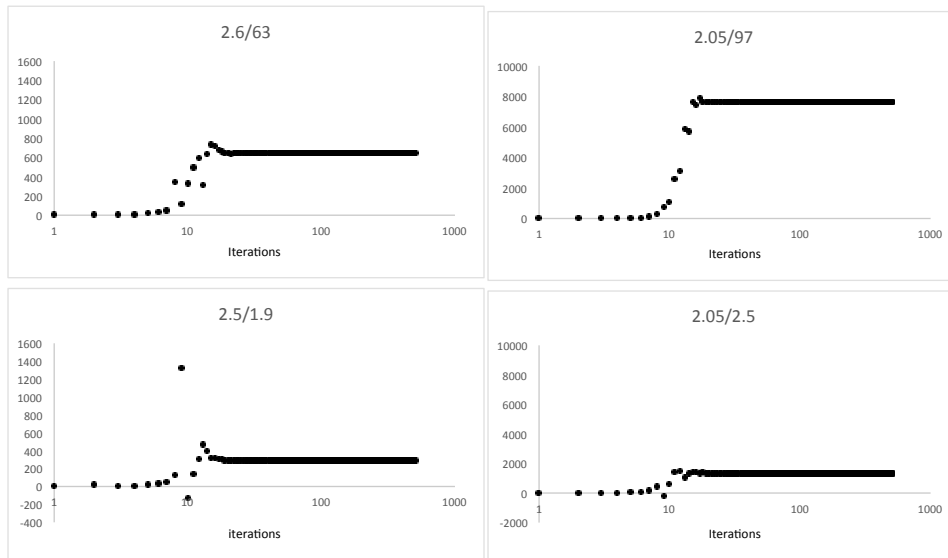


Figure 3A. Tissue specific simulated alloreactive T cell counts in recipients of MRD (Black line) and unrelated donors (Blue line). These values represent the sum of the entire T cell vector responding to the alloreactivity operator matrix of mHA-HLA complexes for a specific organ, including the negative values

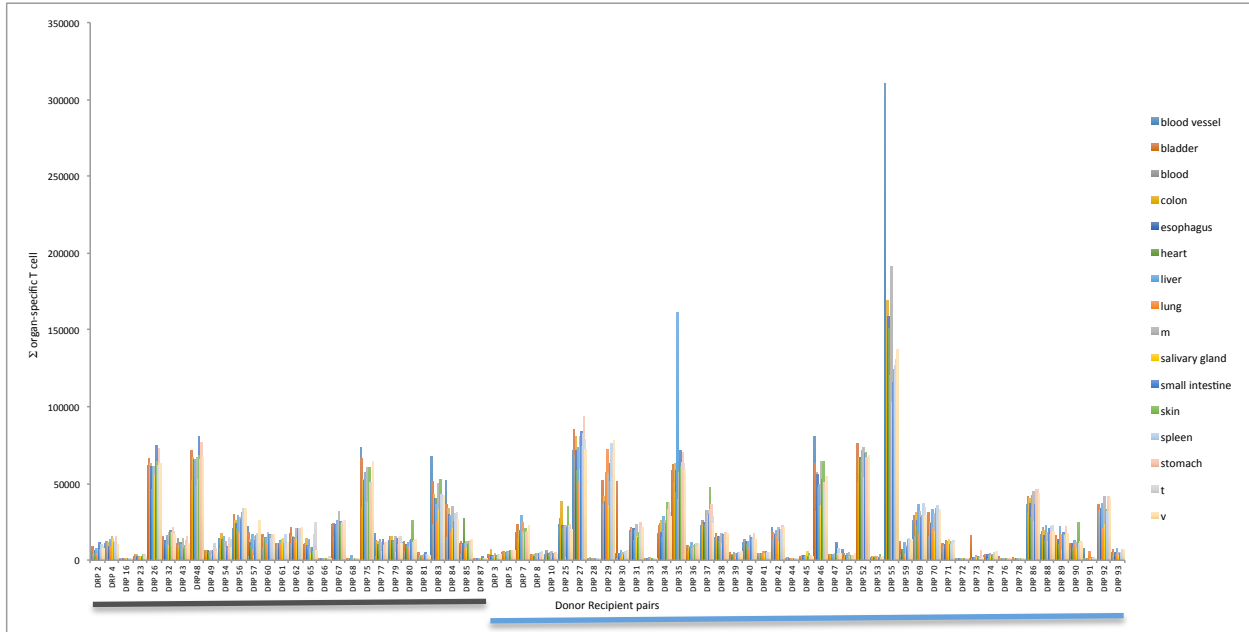
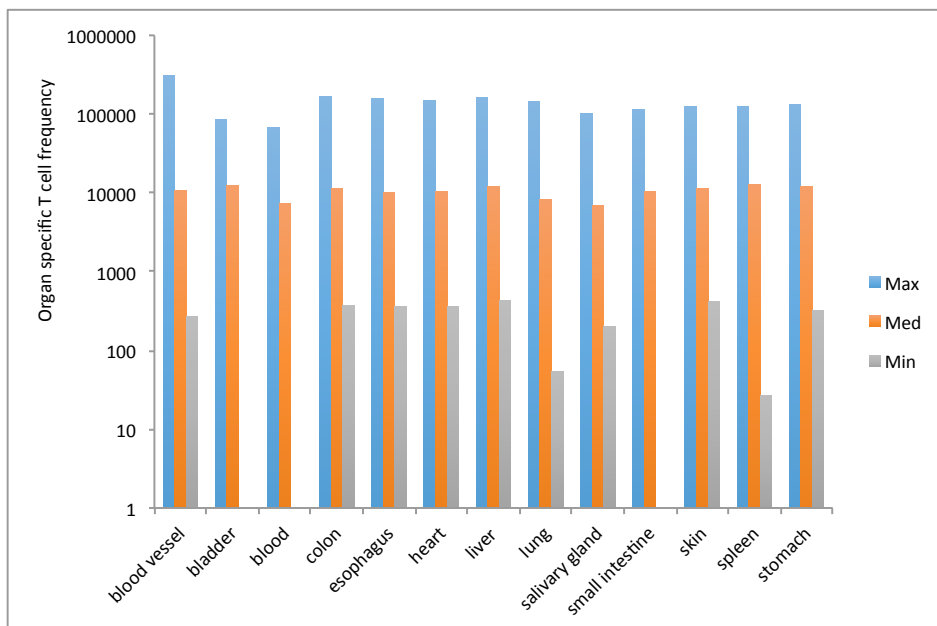


Figure 3B & 3C. Variation in the simulated alloreactive T cell counts observed for each organ examined between patients (3B) and within patients (3C). Note Log scale used in Figure 3B, but not in 3C (Y axis truncated at 130000).

3B.



3C.

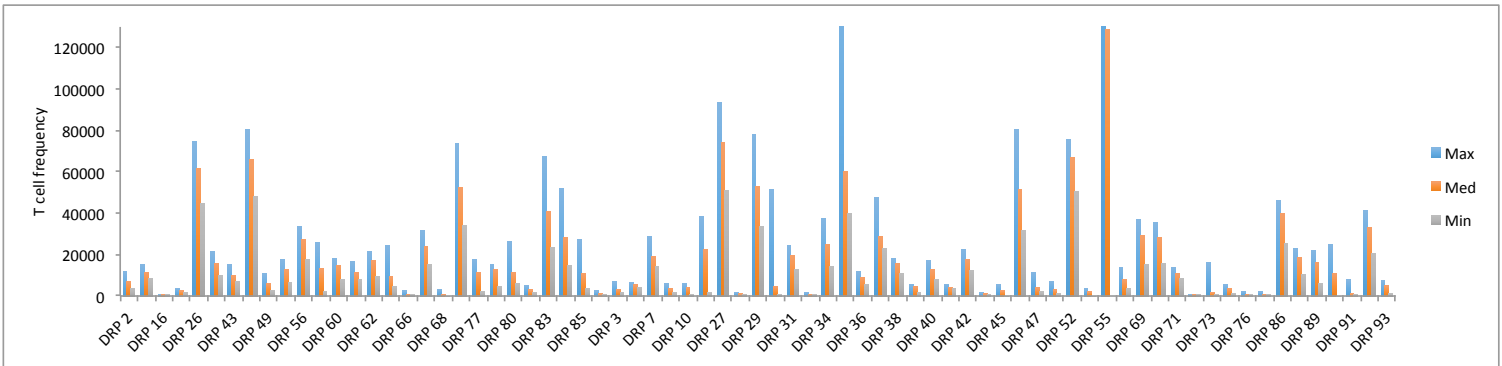


Figure 3D. Cumulative, simulated alloreactive T cell counts in recipients of MRD (Black line) and unrelated donors (Blue line)

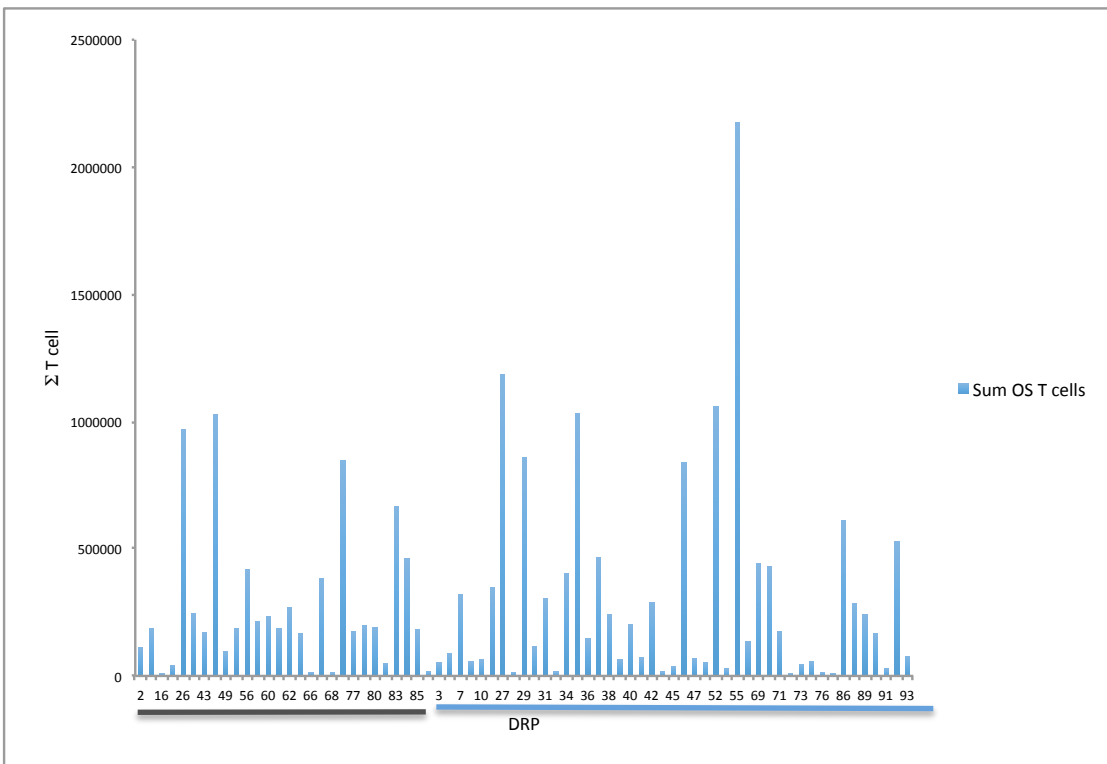
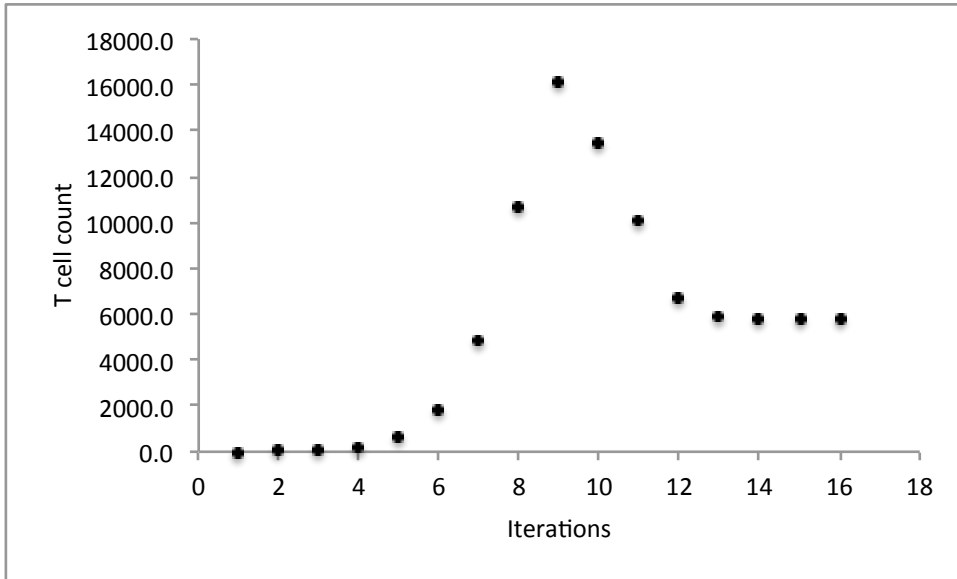
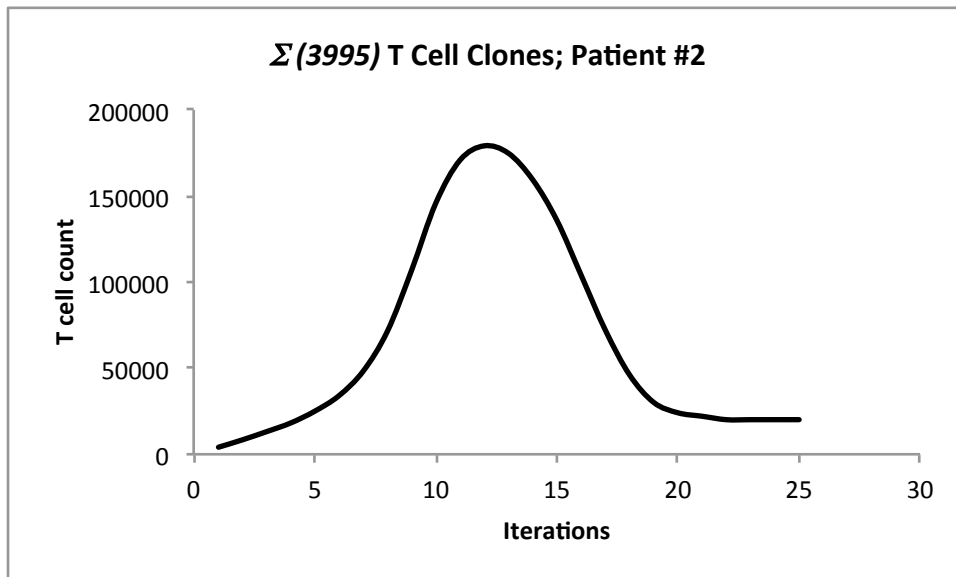


Figure 4: Alloreactivity model. Dot product of APC and T cell vectors recapitulates familiar antigen-challenge driven T cell proliferation response curve. A. Single T cell clone, B. Entire repertoire. C. Model illustrating the interaction between APC and T cells.

4A.



4B.



4C.

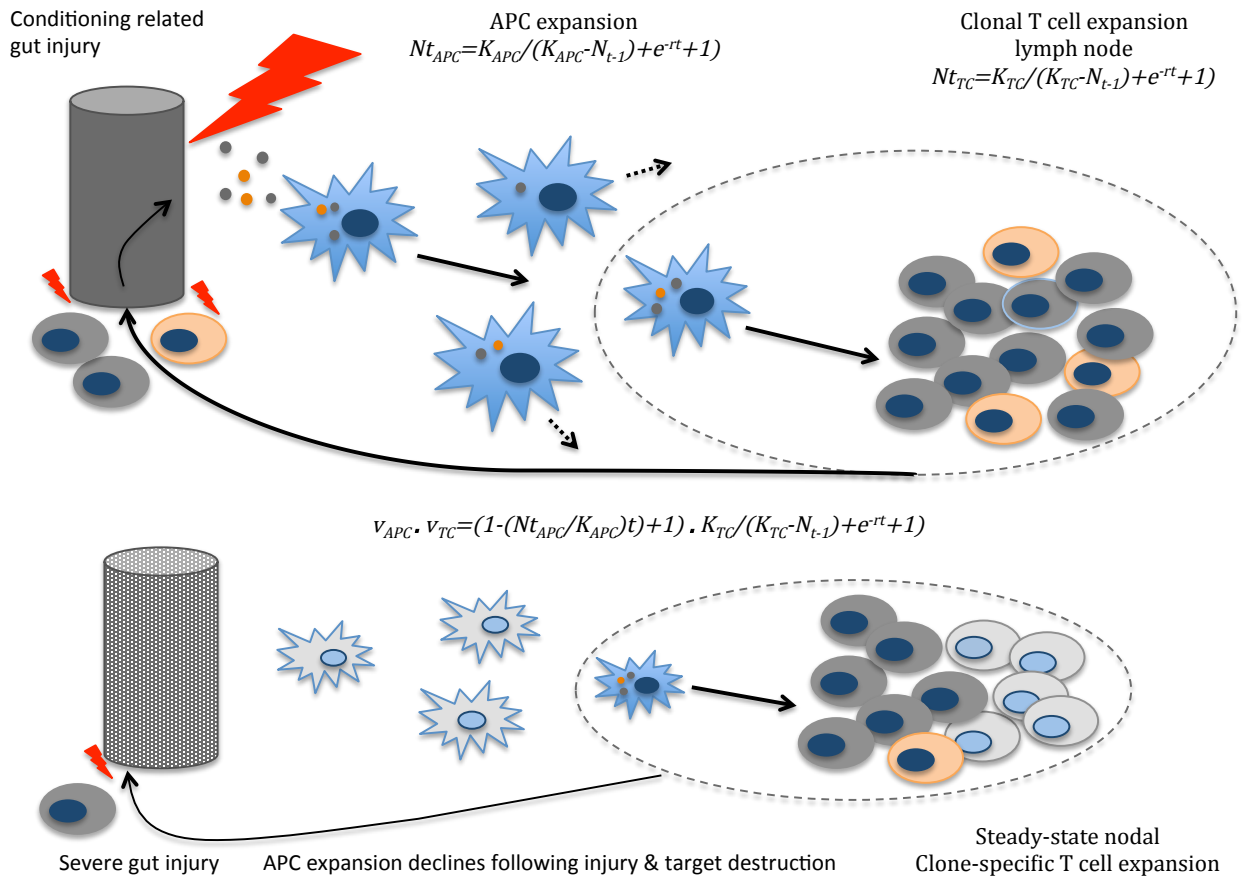
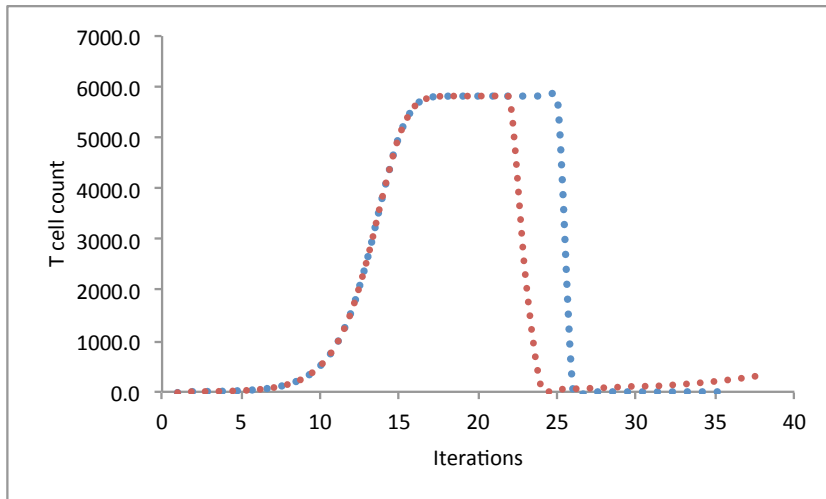


Figure 5. Modeling the effect of Treg on effector T cell growth: in the red curve r reduced at 21st iteration from 1 to 0.25; T cell population drops but then recovers slowly. In the blue curve r reduced at 25th iteration from 1 to 0.25 with direction reversal (from $-$ to $+$), signifying anti-inflammatory effect supersedes pro-inflammatory effect.



Tables.**Table 1.** Exome sequencing and peptide results by donor type (n=77)

	Related^a (n=27)	Unrelated (n=50)	P-value^b
Exome sequencing SNP differences			
Synonymous	2,751	4,821	<0.01
Nonsynonymous	2,490	4,287	<0.01
Conservative	855	1,476	<0.01
Non-conservative	1,635	2,811	<0.01
HLA-Presented Peptides			
Peptides	44,214	77,025	<0.01
Strong Binders	838	1,160	<0.01
Presented Peptides	3,626	5,386	<0.01
Percent of Strong Binders	1.9	1.5	0.03
Percent of Presented Peptides	8.3	7.1	0.05
Strong Binders/Presented Peptides	22.6	21.1	0.08

^aExcludes haploidentical patient^bMean values compared using t-test for Equality of Means

Supplementary Table 1. Patient characteristics, excluding haploidentical DRP

Supplemental Table 1. Patient Characteristics, n (%)	
Total Transplants	77 (100)
Gender	
Male/Female	43 (55.8)/34 (44.2)
Patient Age	
Median (range)	55.6 (21-73)
	Total
Age Distribution	
	<40 12 (16)
	40-59 43 (56)
	≥60 22 (29)
Donor	
	MRD 26 (34)
	MUD 41 (53)
	MMRD 1 (1)
	MMUD 9 (12)
Stem Cell Source	
	Bone Marrow 7 (9)
	Peripheral Blood 70 (91)
Diagnosis	
	Acute lymphoid leukemia 5 (6)
	Acute myeloid leukemia 29 (38)
	Chronic lymphocytic leukemia and lymphomas 15 (19)
	Multiple myeloma 4 (5)
	Myelodysplastic syndromes 24 (31)
Conditioning Regimen	
	Anti-thymocyte globulin (ATG) 62 (81)
	Reduced Intensity 46 (60)
	ATG/TBI 19 (25)
	Busulfan/Fludarabine 27 (35)
	Fludarabine/Melphalan 2 (77)
	Myeloablative 31 (40)
	Busulfan/Cyclophosphamide 17 (22)
	Cyclophosphamide/TBI 11 (14)
	Etoposide/TBI 1 (1)
GVHD prophylaxis	
	Cyclosporin A/Methotrexate 16 (21)
	Cyclosporin A/MMF 4 (5)
	Tacrolimus/Methotrexate 34 (44)
	Tacrolimus/MMF 23 (30)
GVHD, Overall	
	Acute, Grades I-II 20 (26)
	Acute, Grades III-IV 14 (18)
	Chronic 39 (51)
	Both, Acute + Chronic 25 (32)

Supplementary Table 2: Expected T cell counts per donor type by organ (presented in 1,000s of cells)

Table 2				
	MRD (N=27)		MUD (N=45)	
	Mean	SD	Mean	SD
Salivary Glands	13.8	14.9	14.0	20.0
Colon	18.4	18.1	20.2	30.1
Esophagus	17.2	17.8	18.6	28.1
Small Intestines	19.1	20.3	19.9	25.7
Stomach	19.6	19.5	21.1	27.3
Liver	18.4	17.8	22.6	32.1
Lung	12.9	12.9	16.5	25.6
Skin	19.3	19.6	20.9	25.9
Total	138.8	139.3	154.8	210.5
Variance Measures				
Standard Deviation	3.6	2.8	4.7	6.8
Minimum	22.7	21.0	27.3	37.2
Maximum	11.8	13.1	12.8	19.3
Range	10.9	8.7	14.4	21.1

Supplementary Table 3. Expected T cell counts by organ in patients with and without GVHD (presented in 1,000s of cells)

Table 3						
	Overall (N = 73)		No GVHD (N=26)		GVHD (N=47)	
	Mean	SD	Mean	SD	Mean	SD
Salivary Glands	13.7	18.1	10.3	11.9	15.6	20.6
Colon	19.3	26.0	15.3	15.1	21.4	30.3
Esophagus	17.9	24.5	13.6	14.4	20.2	28.5
Small Intestines*	19.3	23.6	14.4	14.9	22.1	27.0
Stomach	20.3	24.4	15.5	15.9	22.9	27.9
Liver	20.8	27.5	16.5	15.9	23.1	32.1
Lung	15.0	21.6	11.4	12.7	16.9	25.1
Skin	20.0	23.6	16.1	16.9	22.2	26.5
Total*	146.7	185.1	113.1	114.9	165.7	213.8
*Indicates sample sizes of 72 for overall and 46 for GVHD group due to a missing value						

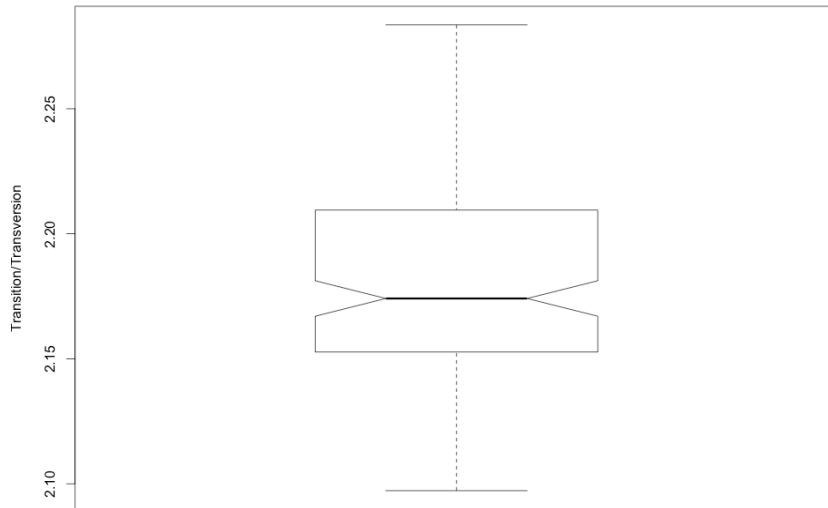
Supplementary Table 4. Estimated hazards ratios, 95% confidence intervals and p-values from Cox-proportional hazards models of t-cell counts and GVHD classification

Table 4			
	Hazard Ratio*	95% CI	p-value
Salivary Glands	1.01	0.99, 1.03	0.1184
Colon	1.01	0.99, 1.02	0.1479
Esophagus	1.01	0.99, 1.02	0.1039
Small Intestines	1.01	0.99, 1.02	0.0946
Stomach	1.01	0.99, 1.02	0.1055
Liver	1.01	0.99, 1.02	0.0546
Lung	1.01	0.99, 1.02	0.1248
Skin	1.01	0.99, 1.02	0.1442
Total	1.00	0.99, 1.01	0.0976
Standard Deviation	1.08	1.01, 1.15	0.0275
Minimum	1.01	0.99, 1.03	0.1049
Maximum	1.01	1.00, 1.02	0.0462
Range	1.02	1.00, 1.05	0.0276
*Hazard ratio based on t-cell counts expressed in 1,000s			

Supplementary Table 5. Estimated hazards ratios, 95% confidence intervals and p-values from Cox-proportional hazards models of t-cell counts and acute and chronic GVHD classification

Table 5						
	Hazard Ratio*	Acute GVHD			Chronic GVHD	
		95% CI	p-value	Hazard Ratio*	95% CI	p-value
Salivary Glands	1.01	0.99, 1.03	0.3806	1.01	0.99, 1.03	0.1090
Colon	1.01	0.99, 1.02	0.4175	1.01	0.99, 1.02	0.2394
Esophagus	1.01	0.99, 1.02	0.3379	1.01	0.99, 1.02	0.1633
Small Intestines	1.01	0.99, 1.02	0.3880	1.01	0.99, 1.03	0.0788
Stomach	1.01	0.99, 1.02	0.4788	1.01	0.99, 1.02	0.1321
Liver	1.01	0.99, 1.02	0.1752	1.01	1.00, 1.03	0.0411
Lung	1.01	0.99, 1.02	0.2664	1.01	0.99, 1.03	0.2520
Skin	1.01	0.99, 1.02	0.3851	1.01	0.99, 1.02	0.1732
Total	1.00	0.99, 1.00	0.3290	1.00	1.00, 1.00	0.1202
Standard Deviation	1.07	0.99, 1.15	0.0618	1.08	1.01, 1.16	0.0404
Minimum	1.01	0.99, 1.03	0.3492	1.01	0.99, 1.03	0.1520
Maximum	1.01	0.99, 1.02	0.1526	1.01	0.99, 1.02	0.0586
Range	1.02	0.99, 1.05	0.0539	1.03	1.01, 1.05	0.0266
*Hazard ratio based on t-cell counts expressed in 1,000s						

Supplementary Figure 1: Transition/transversion ratio for the WES data from all the patients.



Acknowledgements. This work was supported by Massey Pilot Project Grant and an award from Virginia's Commonwealth Health Research Board (PI: MN). VK performed bioinformatic analysis of the sequencing data to identify unique peptides and their HLA binding affinity, as well as tissue expression. BA, SS wrote the program for performing calculations in MATLAB and performed vector-operator calculations presented in this paper. AS, DJK and TS collected and verified clinical outcome data. AS and RS performed statistical analysis. MS performed sequencing on samples identified and procured by CR. AS, CH and MJ-L created data files with unique peptides and HLA IC50 values. All the authors contributed to writing the manuscript.

References:

1. Kröger N, Solano C, Wolschke C, Bandini G, Patriarca F, Pini M, Nagler A, Selleri C, Risitano A, Messina G, Bethge W, Pérez de Oteiza J, Duarte R, Carella AM, Cimminiello M, Guidi S, Finke J, Mordini N, Ferra C, Sierra J, Russo D, Petrini M, Milone G, Benedetti F, Heinzelmann M, Pastore D, Jurado M, Terruzzi E, Narni F, Völp A, Ayuk F, Ruutu T, Bonifazi F. Antilymphocyte Globulin for Prevention of Chronic Graft-versus-Host Disease. *N Engl J Med*. 2016 Jan 7;374(1):43-53.
2. Ringdén O, Labopin M, Ciceri F, Velardi A, Bacigalupo A, Arcese W, Ghavamzadeh A, Hamladji RM, Schmid C, Nagler A, Mohty M. Is there a stronger graft-versus-leukemia effect using HLA-haploidentical donors compared with HLA-identical siblings? *Leukemia*. 2016 Feb;30(2):447-55.
3. Ciurea SO, Zhang MJ, Bacigalupo AA, Bashey A, Appelbaum FR, Aljritawi OS, Armand P, Antin JH, Chen J, Devine SM, Fowler DH, Luznik L, Nakamura R, O'Donnell PV, Perales MA, Pingali SR, Porter DL, Riches MR, Ringdén OT, Rocha V, Vij R, Weisdorf DJ, Champlin RE, Horowitz MM, Fuchs EJ, Eapen M. Haploidentical transplant with posttransplant cyclophosphamide vs matched unrelated donor transplant for acute myeloid leukemia. *Blood*. 2015 Aug 20;126(8):1033-40.
4. Holtick U, Albrecht M, Chemnitz JM, Theurich S, Shimabukuro-Vornhagen A, Skoetz N, Scheid C, von Bergwelt-Baildon M. Comparison of bone marrow versus peripheral blood allogeneic hematopoietic stem cell transplantation for hematological malignancies in adults - a systematic review and meta-analysis. *Crit Rev Oncol Hematol*. 2015 May;94(2):179-88.
5. Eapen M, Logan BR, Horowitz MM, Zhong X, Perales MA, Lee SJ, Rocha V, Soiffer RJ, Champlin RE. Bone marrow or peripheral blood for reduced-intensity conditioning unrelated donor transplantation. *J Clin Oncol*. 2015 Feb 1;33(4):364-9.
6. Inamoto Y, Flowers ME, Appelbaum FR, Carpenter PA, Deeg HJ, Furlong T, Kiem HP, Mielcarek M, Nash RA, Storb RF, Witherspoon RP, Storer BE, Martin PJ. A retrospective comparison of tacrolimus versus cyclosporine with methotrexate for immunosuppression after allogeneic hematopoietic cell transplantation with mobilized blood cells. *Biol Blood Marrow Transplant*. 2011 Jul;17(7):1088-92.
7. Kanda Y, Kobayashi T, Mori T, Tanaka M, Nakaseko C, Yokota A, Watanabe R, Kako S, Kakahana K, Kato J, Tanihara A, Doki N, Ashizawa M, Kimura SI, Kikuchi M, Kanamori H, Okamoto S; Kanto Study Group for Cell Therapy. A randomized controlled trial of cyclosporine and tacrolimus with strict control of blood concentrations after unrelated bone marrow transplantation. *Bone Marrow Transplant*. 2016 Jan;51(1):103-9.
8. Brunstein CG, Fuchs EJ, Carter SL, Karanes C, Costa LJ, Wu J, Devine SM, Wingard JR, Aljritawi OS, Cutler CS, Jagasia MH, Ballen KK, Eapen M, O'Donnell PV; Blood and Marrow Transplant Clinical Trials Network. Alternative donor transplantation after reduced intensity conditioning: results of parallel phase 2 trials using partially HLA-mismatched related bone marrow or unrelated double umbilical cord blood grafts. *Blood*. 2011 Jul 14;118(2):282-8.

-
9. El-Cheikh J, Crocchiolo R, Furst S, Bramanti S, Sarina B, Granata A, Vai A, Lemarie C, Faucher C, Mohty B, Harbi S, Bouabdallah R, Vey N, Santoro A, Chabannon C, Castagna L, Blaise D. Unrelated cord blood compared with haploidentical grafts in patients with hematological malignancies. *Cancer*. 2015 Jun 1;121(11):1809-16.
 10. Petersen SL. Alloreactivity as therapeutic principle in the treatment of hematologic malignancies. Studies of clinical and immunologic aspects of allogeneic hematopoietic cell transplantation with nonmyeloablative conditioning. *Dan Med Bull*. 2007 May;54(2):112-39.
 11. Toor AA, Sabo RT, Roberts CH, Moore BL, Salman SR, Scalora AF, Aziz MT, Shubar Ali AS, Hall CE, Meier J, Thorn RM, Wang E, Song S, Miller K, Rizzo K, Clark WB, McCarty JM, Chung HM, Manjili MH, Neale MC. Dynamical System Modeling of Immune Reconstitution after Allogeneic Stem Cell Transplantation Identifies Patients at Risk for Adverse Outcomes. *Biol Blood Marrow Transplant*. 2015 Jul;21(7):1237-45.
 12. Bayraktar UD, Milton DR, Guindani M, Rondon G, Chen J, Al-Atrash G, Rezvani K, Champlin R, Ciurea SO. Optimal Threshold and Time of Absolute Lymphocyte Count Assessment for Outcome Prediction after Bone Marrow Transplantation. *Biol Blood Marrow Transplant*. 2016 Mar;22(3):505-13.
 13. Storb R, Gyurkocza B, Storer BE, Maloney DG, Sorrow ML, Mielcarek M, Martin PJ, Sandmaier BM. Allogeneic hematopoietic cell transplantation following minimal intensity conditioning: predicting acute graft-versus-host disease and graft-versus-tumor effects. *Biol Blood Marrow Transplant*. 2013 May;19(5):792-8.
 14. Meier J, Roberts C, Avent K, Hazlett A, Berrie J, Payne K, Hamm D, Desmarais C, Sanders C, Hogan KT, Archer KJ, Manjili MH, Toor AA. Fractal organization of the human T cell repertoire in health and after stem cell transplantation. *Biol Blood Marrow Transplant*. 2013 Mar;19(3):366-77.
 15. Bolkhovskaya OV, Zorin DY, Ivanchenko MV. Assessing T cell clonal size distribution: a non-parametric approach. *PLoS One*. 2014 Oct 2;9(9):e108658.
 16. Sampson JK, Sheth NU, Koparde VN, Scalora AF, Serrano MG, Lee V, Roberts CH, Jameson-Lee M, Ferreira-Gonzalez A, Manjili MH, Buck GA, Neale MC, Toor AA. Whole exome sequencing to estimate alloreactivity potential between donors and recipients in stem cell transplantation. *Br J Haematol*. 2014 Aug;166(4):566-70.
 17. Jameson-Lee M, Koparde V, Griffith P, Scalora AF, Sampson JK, Khalid H, Sheth NU, Batalo M, Serrano MG, Roberts CH, Hess ML, Buck GA, Neale MC, Manjili MH, Toor AA. In silico Derivation of HLA-Specific Alloreactivity Potential from Whole Exome Sequencing of Stem-Cell Transplant Donors and Recipients: Understanding the Quantitative Immunobiology of Allogeneic Transplantation. *Front Immunol*. 2014 Nov 6;5:529.
 18. Abdul Razzaq B, Scalora A, Koparde VN, Meier J, Mahmood M, Salman S, Jameson-Lee M, Serrano MG, Sheth N, Voelkner M, Kobulnicky DJ, Roberts CH, Ferreira-Gonzalez A, Manjili MH, Buck GA, Neale MC, Toor AA. Dynamical System Modeling to Simulate Donor T Cell Response to Whole Exome Sequencing-Derived Recipient Peptides Demonstrates Different Alloreactivity Potential in HLA-Matched and -Mismatched Donor-Recipient Pairs. *Biol Blood Marrow Transplant*. 2016 May;22(5):850-61.
 19. Pidala J, Wang T, Haagenson M, Spellman SR, Askar M, Battiwalla M, Baxter-Lowe LA, Bitan M, Fernandez-Viña M, Gandhi M, Jakubowski AA, Maiers M, Marino SR, Marsh SG, Oudshoorn M, Palmer J, Prasad VK, Reddy V,

-
- Ringden O, Saber W, Santarone S, Schultz KR, Setterholm M, Trachtenberg E, Turner EV, Woolfrey AE, Lee SJ, Anasetti C. Amino acid substitution at peptide-binding pockets of HLA class I molecules increases risk of severe acute GVHD and mortality. *Blood*. 2013 Nov 21;122(22):3651-8.
20. May RM. Simple mathematical models with very complicated dynamics. *Nature*. 1976 Jun 10; 261 (5560): 459-67.
21. Morrison F. A classification scheme for dynamic systems, pp 165, in *The Art of Modeling Dynamic Systems: Forecasting for Chaos, Randomness and Determinism*. (2008) Dover publications, Mineola, NY.
22. Susskind L & Friedman A. "Mathematical Interlude: Vector Spaces" in *Quantum Mechanics. The Theoretical Minimum*. New York, NY: Basic Books (2014) p. 24-28
23. Susskind L & Friedman A. "Mathematical Interlude: Linear Operators" in *Quantum Mechanics. The Theoretical Minimum*. New York, NY: Basic Books (2014) p. 52-56
24. Murray JD. *Competition Models: Principle of Competitive Exclusion in Mathematical Biology*. New York, NY: Springer (2002) p. 94
25. Gilpin ME, Ayala FJ. Global models of growth and competition. *Proc Natl Acad Sci U S A*. 1973 Dec;70(12):3590-3.
26. Ringdén O, Labopin M, Solders M, Beelen D, Arnold R, Ehninger G, Milpied N, Niederwieser D, Hamladji RM, Kyrz-Krzemien S, Ganser A, Socié G, Stelljes M, Volin L, Craddock C, Mohty M; Acute Leukaemia Working Party of the European Group for Blood and Marrow Transplantation.. Who is the best hematopoietic stem-cell donor for a male patient with acute leukemia? *Transplantation*. 2014 Sep 15;98(5):569-77.
27. Morishima Y, Kashiwase K, Matsuo K, Azuma F, Morishima S, Onizuka M, Yabe T, Murata M, Doki N, Eto T, Mori T, Miyamura K, Sao H, Ichinohe T, Saji H, Kato S, Atsuta Y, Kawa K, Koderia Y, Sasazuki T; Japan Marrow Donor Program.. Biological significance of HLA locus matching in unrelated donor bone marrow transplantation. *Blood*. 2015 Feb 12;125(7):1189-97.
28. Valcárcel D, Sierra J, Wang T, Kan F, Gupta V, Hale GA, Marks DI, McCarthy PL, Oudshoorn M, Petersdorf EW, Ringdén O, Setterholm M, Spellman SR, Waller EK, Gajewski JL, Marino SR, Senitzer D, Lee SJ. One-antigen mismatched related versus HLA-matched unrelated donor hematopoietic stem cell transplantation in adults with acute leukemia: Center for International Blood and Marrow Transplant Research results in the era of molecular HLA typing. *Biol Blood Marrow Transplant*. 2011 May;17(5):640-8.
29. Petersdorf EW, Malkki M, Gooley TA, Martin PJ, Guo Z. MHC haplotype matching for unrelated hematopoietic cell transplantation. *PLoS Med*. 2007 Jan;4(1):e8.
30. Woolfrey A, Klein JP, Haagensohn M, Spellman S, Petersdorf E, Oudshoorn M, Gajewski J, Hale GA, Horan J, Battiwalla M, Marino SR, Setterholm M, Ringden O, Hurley C, Flomenberg N, Anasetti C, Fernandez-Vina M, Lee SJ. HLA-C antigen mismatch is associated with worse outcome in unrelated donor peripheral blood stem cell transplantation. *Biol Blood Marrow Transplant*. 2011 Jun;17(6):885-92.
31. Kröger N, Solano C, Wolschke C, Bandini G, Patriarca F, Pini M, Nagler A, Sella C, Risitano A, Messina G, Bethge W, Pérez de Oteiza J, Duarte R, Carella AM, Cimminiello M, Guidi S, Finke J, Mordini N, Ferra C, Sierra J, Russo D, Petrini M, Milone G, Benedetti F, Heinzelmann M, Pastore D, Jurado M, Terruzzi E, Narni F, Völp A, Ayuk F, Ruutu T,

Bonifazi F. Antilymphocyte Globulin for Prevention of Chronic Graft-versus-Host Disease. *N Engl J Med.* 2016 Jan 7;374(1):43-53.

32. Armand P, Kim HT, Sainvil MM, Lange PB, Giardino AA, Bachanova V, Devine SM, Waller EK, Jagirdar N, Herrera AF, Cutler C, Ho VT, Koreth J, Alyea EP, McAfee SL, Soiffer RJ, Chen YB, Antin JH. The addition of sirolimus to the graft-versus-host disease prophylaxis regimen in reduced intensity allogeneic stem cell transplantation for lymphoma: a multicentre randomized trial. *Br J Haematol.* 2016 Apr;173(1):96-104.

33. Koreth J, Kim HT, Lange PB, Bindra B, Reynolds CG, Chammass MJ, Armand P, Cutler CS, Ho VT, Grotzbecker B, Nikiforow S, Ritz J, Blazar BR, Soiffer RJ, Antin JH, Alyea EP 3rd. A Bortezomib-Based Regimen Offers Promising Survival and Graft-versus-Host Disease Prophylaxis in Myeloablative HLA-Mismatched and Unrelated Donor Transplantation: A Phase II Trial. *Biol Blood Marrow Transplant.* 2015 Nov;21(11):1907-13.

34. Anasetti C, Logan BR, Lee SJ, Waller EK, Weisdorf DJ, Wingard JR, Cutler CS, Westervelt P, Woolfrey A, Couban S, Ehninger G, Johnston L, Maziarz RT, Pulsipher MA, Porter DL, Mineishi S, McCarty JM, Khan SP, Anderlini P, Bensinger WI, Leitman SF, Rowley SD, Bredeson C, Carter SL, Horowitz MM, Confer DL; Blood and Marrow Transplant Clinical Trials Network.. Peripheral-blood stem cells versus bone marrow from unrelated donors. *N Engl J Med.* 2012 Oct 18;367(16):1487-96.

35. Czerw T, Labopin M, Schmid C, Cornelissen JJ, Chevallier P, Blaise D, Kuball J, Vigouroux S, Garban F, Lioure B, Fegueux N, Clement L, Sandstedt A, Maertens J, Guillerm G, Bordessoule D, Mohty M, Nagler A. High CD3+ and CD34+ peripheral blood stem cell grafts content is associated with increased risk of graft-versus-host disease without beneficial effect on disease control after reduced-intensity conditioning allogeneic transplantation from matched unrelated donors for acute myeloid leukemia - an analysis from the Acute Leukemia Working Party of the European Society for Blood and Marrow Transplantation. *Oncotarget.* 2016 May 10;7(19):27255-66.

36. Freund, JE. Introduction to Probability. Probabilities, p 33-59. Dover Publications, 1973.

37. Benjamin, A. The Magic of Mathematics; Solving For X And Figuring Out Why. The Magic of Counting, p71-99. Basic Books, 2015.

38. Petersdorf EW, Gooley TA, Malkki M, Bacigalupo AP, Cesbron A, Du Toit E, Ehninger G, Egeland T, Fischer GF, Gervais T, Haagenon MD, Horowitz MM, Hsu K, Jindra P, Madrigal A, Oudshoorn M, Ringdén O, Schroeder ML, Spellman SR, Tiercy JM, Velardi A, Witt CS, O'Huigin C, Apps R, Carrington M; International Histocompatibility Working Group in Hematopoietic Cell Transplantation.. HLA-C expression levels define permissible mismatches in hematopoietic cell transplantation. *Blood.* 2014 Dec 18;124(26):3996-4003.

39. Petersdorf EW, Malkki M, O'Huigin C, Carrington M, Gooley T, Haagenon MD, Horowitz MM, Spellman SR, Wang T, Stevenson P. High HLA-DP Expression and Graft-versus-Host Disease. *N Engl J Med.* 2015 Aug 13;373(7):599-609.

40. Kaech SM, Cui W. Transcriptional control of effector and memory CD8+ T cell differentiation. *Nat Rev Immunol.* 2012 Nov;12(11):749-61.

41. Russ BE, Prier JE, Rao S, Turner SJ. T cell immunity as a tool for studying epigenetic regulation of cellular differentiation. *Front Genet.* 2013 Nov 12;4:218.

42. Bevan MJ. Helping the CD8(+) T-cell response. *Nat Rev Immunol.* 2004 Aug;4(8):595-602.

43. Pandiyan P, Zheng L, Lenardo MJ. The Molecular Mechanisms of Regulatory T Cell Immunosuppression. *Frontiers in Immunology.* 2011;2:60. doi:10.3389/fimmu.2011.00060.